arXiv:0901.3046v2 [hep-th] 1 Apr 2009

TIT/HEP-592
January, 2009
revised version

Discretized Minimal Surface and the BDS Conjecture in $\mathcal{N} = 4$ Super Yang-Mills Theory at Strong Coupling

Suguru Dobashi[1] and Katsushi Ito[2]

[1] *Department of Accelerator and Medical Physics,*
National Institute of Radiological Sciences,
4-9-1 Anagawa, Inage-ku, Chiba 263-8555, Japan

[2] *Department of Physics*
Tokyo Institute of Technology
2-12-1, Ookayama, Meguro-ku, Tokyo, 152-8551, Japan

Abstract

We construct numerically the minimal surface in AdS spacetime surrounded by the light-like segments, which are dual to the 4, 6 and 8-point gluon scattering amplitudes in $N = 4$ super Yang-Mills theory. We evaluate the area of the minimal surface in the radial cut-off regularization and compare these areas with the formula conjectured by Bern, Dixon and Smirnov (BDS), which is modified by the remainder function of cross-ratios of external momenta for $n(\geq 6)$-point amplitudes. In our momentum configuration cross-ratios are constant. We calculate the difference of areas with different conformal boost parameters, which is independent of the remainder function, and find that its dependence on the boost parameter is numerically consistent with the BDS formula.

1 Introduction

One of recent important developments in study of the AdS/CFT correspondence is the duality between gluon scattering amplitudes in $\mathcal{N} = 4$ super Yang-Mills theory and the area of the minimal surface in AdS spacetime surrounded by the closed light-like Wilson loops. From the duality one can compute the gluon scattering amplitudes at strong coupling. In the case of the 4-point amplitude, Alday and Maldacena [1] showed that the dimensionally regularized area agrees with the formula conjectured by Bern, Dixon and Smirnov (BDS) [2] based on the perturbative analysis. See [3, 4, 5, 6, 7, 8, 9] for further developments.

The duality between gluon scattering amplitudes and Wilson loops is shown to hold at weak coupling [10], which implies that the amplitude is invariant under dual conformal symmetry in momentum space [11]. In superstring theory, this symmetry is interpreted as the symmetry of AdS spacetime and invariance of the action under the combination of bosonic and fermionic T-duality[12]. The anomalous conformal Ward identity constrains the structure of the 4 and 5-point amplitudes, which agrees with the BDS formula. But for higher $n(\geq 6)$-point amplitudes there arises some ambiguities in the finite remainder part of the amplitude which can be written in terms of the conformal invariant cross-ratio of the external gluon momenta [11].

In fact, the explicit calculations of the two-loop 6-point gluon scattering amplitude and the hexagon Wilson loop [13] shows that they agree with each other but differ from the BDS formula by finite term, which depends on three independent cross-ratios of the Mandelstam variables. This discrepancy from the BDS ansatz was also observed at strong coupling by studying zigzag rectangular [6] and a wavy circular Wilson lines [7]. But the precise evaluation of the finite deviation from the BDS formula is difficult to obtain since the exact solution of the minimal surface for higher-point amplitudes is not yet known.

In a previous paper [9], we constructed the minimal surfaces corresponding to the 4, 6 and 8 point amplitudes numerically and evaluate the area in the radial cut-off regularization. The light-like segments of the boundary is the same as the cut and glue type surface [8]. We showed that the numerical solutions differ from the cut and glue type surface and the area is consistent with the IR behavior of the amplitude. In this paper we will study

the area of the discretized surfaces for the 6 and 8-point amplitudes by applying conformal transformation and compare the area to the conjectured BDS formula numerically. This analysis gives a test of the duality between gluon scattering amplitudes and the Wilson loops at strong coupling.

This paper is organized as follows: In section 2, we review the radial cut-off regularization and a numerical approach to the construction of the minimal surface. In section 3, we apply the conformal transformation to the 4-point amplitudes and compare it with the exact formula of the area in the radial cut-off regularization. We propose a method to compare the numerical data with the BDS formula without using the exact formula of the area in the radial cut-off regularization. In section 4, we apply this method to the minimal surfaces corresponding to the 6 and 8-point amplitudes and compare the numerical solutions with the BDS formula. Section 5 is devoted to discussion.

2 Radial cut-off regularization and discretized minimal surface

In this section we review the radial cut-off regularization of the minimal surface in AdS spacetime and a numerical approach to get discretized version of minimal surface. We consider the surface which is surrounded by the curve C_n made of light-like segments $\Delta y^\mu = 2\pi p_i^\mu$. This corresponds to the n-point gluon amplitude with on-shell momenta p_i ($p_i^2 = 0$, $i = 1, \cdots, n$). The coordinates y^μ ($\mu = 0, 1, 2, 3$) and the radial coordinate r are the Poincaré coordinates in AdS_5 spacetime with the metric

$$ds^2 = R^2 \frac{dy^\mu dy_\mu + dr^2}{r^2}, \tag{2.1}$$

and R is the radius of AdS_5. The Nambu-Goto action in the static gauge $y_3 = 0$ is given by

$$S = \frac{R^2}{2\pi} \int dy_1 dy_2 \frac{\sqrt{1 + (\partial_i r)^2 - (\partial_i y_0)^2 - (\partial_1 r \partial_2 y_0 - \partial_2 r \partial_1 y_0)^2}}{r^2}. \tag{2.2}$$

Here ∂_i is the derivative with respect to y_i ($i = 1, 2$). The Euler-Lagrange equations become

$$\partial_i \left(\frac{\partial L}{\partial(\partial_i y_0)} \right) = 0, \quad \partial_i \left(\frac{\partial L}{\partial(\partial_i r)} \right) - \frac{\partial L}{\partial r} = 0, \tag{2.3}$$

where L is the Lagrangian of the action. By solving these non-linear partial differential equations, one obtains the minimal surface $r = r(y_1, y_2)$ and $y_0 = y_0(y_1, y_2)$.

We consider the 4-point amplitude for two incoming particles with momenta p_1 and p_3 and outgoing particles with momenta p_2 and p_4. For the momentum configuration in the (y_0, y_1, y_2)-space

$$2\pi p_1 = (2, 2, 0), \quad 2\pi p_2 = (-2, 0, 2), \quad 2\pi p_3 = (2, -2, 0), \quad 2\pi p_4 = (-2, 0, -2), \tag{2.4}$$

the Wilson loop is represented by the square with corners at $y_1, y_2 = \pm 1$. The boundary condition for the Euler-Lagrange equations is given by

$$r(\pm 1, y_2) = r(y_1, \pm 1) = 0, \quad y_0(\pm 1, y_2) = \pm y_2, \quad y_0(y_1, \pm 1) = \pm y_1. \tag{2.5}$$

Alday and Maldacena [1] found the exact solution of the nonlinear differential equations (2.3), which is given by

$$y_0(y_1, y_2) = y_1 y_2, \quad r(y_1, y_2) = \sqrt{(1 - y_1^2)(1 - y_2^2)}. \tag{2.6}$$

The above solution corresponds to the $s = t$ solution, where s and t are the Mandelstam variables defined by $s = -(p_1 + p_2)^2$ and $t = -(p_2 + p_3)^2$. The general (s, t) solution is obtained by scale and boost transformation of the $s = t$ solution:

$$r' = \frac{ar}{1 + by_0}, \quad y_0' = \frac{a\sqrt{1 + b^2} y_0}{1 + by_0}, \quad y_i' = \frac{a y_i}{1 + by_0}, \tag{2.7}$$

where a is a parameter for the scale transformation and b is a boost parameter. After the conformal transformation, the momenta become

$$\begin{aligned}
2\pi p_1 &= (\frac{2a\sqrt{1 + b^2}}{1 - b^2}, \frac{2a}{1 - b^2}, -\frac{2ab}{1 - b^2}), \\
2\pi p_2 &= (-\frac{2a\sqrt{1 + b^2}}{1 - b^2}, -\frac{2ab}{1 - b^2}, \frac{2a}{1 - b^2}), \\
2\pi p_3 &= (\frac{2a\sqrt{1 + b^2}}{1 - b^2}, -\frac{2a}{1 - b^2}, \frac{2ab}{1 - b^2}), \\
2\pi p_4 &= (-\frac{2a\sqrt{1 + b^2}}{1 - b^2}, \frac{2ab}{1 - b^2}, -\frac{2a}{1 - b^2}).
\end{aligned} \tag{2.8}$$

The Mandelstam variables s and t are given by

$$(2\pi)^2 s = -\frac{8a^2}{(1-b)^2}, \quad (2\pi)^2 t = -\frac{8a^2}{(1+b)^2}. \tag{2.9}$$

Using the dimensional regularization for the Dp-brane ($p = 3 - 2\epsilon$), the area is shown to agree with the BDS formula at strong coupling [1]. In this paper we will use the radial cut-off regularization instead.

2.1 Radial cut-off regularization

In the radial cut-off regularization scheme we introduce a cut-off r_c in the radial direction[3, 9]. For general (s,t) solution, the regularized area is surrounded by the cut-off curve C in the (y_1, y_2)-plane:

$$r_c^2 = a^2(1-y_1^2)(1-y_2^2)\frac{1}{(1+by_1y_2)^2}. \tag{2.10}$$

The action is evaluated by substituting the solution (2.6) into (2.2). The result is

$$S_4[r_c, b] = \int_S dy_1 dy_2 \frac{1}{(1-y_1^2)(1-y_2^2)}. \tag{2.11}$$

where S is the region surrounded by the curve C.

We can put $a = 1$ by rescaling $r_c \to r_c a$. For fixed y_1, y_2 takes the value in the range $y_2^{c-} \le y_2 \le y_2^{c+}$, where

$$y_2^{c\pm} = \frac{-br_c^2 y_1 \pm \sqrt{(1-y_1^2)(1-y_1^2-r_c^2+b^2r_c^2y_1^2)}}{1-y_1^2+b^2r_c^2y_1^2}. \tag{2.12}$$

In (2.11), the integral over y_2 yields

$$S_4[r_c, b] = \int_{-\sqrt{\frac{1-r_c^2}{1-b^2r_c^2}}}^{\sqrt{\frac{1-r_c^2}{1-b^2r_c^2}}} dy_1 f(y_1, r_c), \tag{2.13}$$

where

$$f(y_1, r_c) = \frac{1}{1-y_1^2}\frac{1}{2}\log\left(\frac{1+y_2^{c+}}{1-y_2^{c+}}\frac{1-y_2^{c-}}{1+y_2^{c-}}\right). \tag{2.14}$$

Expanding $f(y_1, r_c)$ in r_c we get

$$f(y_1, r_c) = -\frac{1}{1-y_1^2}\log(r_c^2\frac{1-b^2y_1^2}{4(1-y_1^2)}) + O(r_c^2). \tag{2.15}$$

After the integral over y_1 in (2.13), we obtain the action $S[r_c, b]$ in the radial cut-off regularization. We note that $\mathrm{O}(r_c^2)$ terms in (2.13) also contribute a constant term. We then obtain

$$S_4[r_c, b] = \frac{1}{4}\log^2\left(\frac{r_c^2}{-8\pi^2 s}\right) + \frac{1}{4}\log^2\left(\frac{r_c^2}{-8\pi^2 t}\right) - \frac{1}{4}\log^2(\frac{s}{t}) + a_0 + O(r_c^2\log r_c^2). \tag{2.16}$$

Evaluating the constant a_0 numerically up to $O(r_c^n)$ ($n = 500$) terms in (2.15), we get $a_0 = -3.28977$. This shows that the finite term numerically agrees with the BDS formula [2]

$$F_4 = -\frac{1}{2}F_4^{BDS}, \quad F_4^{BDS} = \frac{1}{2}\log^2(\frac{s}{t}) + \frac{2\pi^2}{3}, \tag{2.17}$$

since $\frac{\pi^2}{3} = 3.28987....$

Motivated from the analysis of the 4-point amplitude, the n-point amplitude is expected to have the structure [3, 9]

$$S_n[r_c] = \frac{1}{8}\sum_{i=1}^{n}\left(\log\frac{r_c^2}{-8\pi^2 s_{i,i+1}}\right)^2 + F_n(p_1, \cdots, p_n) + O(r_c^2\log r_c^2), \tag{2.18}$$

where $s_{i,i+1} = -(p_i + p_{i+1})^2$ and $p_{n+1} = p_1$. We have factored out the cusp anomalous dimension in the above formula. The first term in (2.18) characterizes infra-red divergences of the amplitude. The function $F_n(p_1, \cdots, p_n)$ is a finite remainder part of the amplitude and takes the form

$$F_n = -\frac{1}{2}F_n^{BDS} + R_n. \tag{2.19}$$

The term F_n^{BDS} is given by the BDS formula which is written in terms of the Mandelstam variables

$$x_{ij}^2 = t_i^{[j-i]} = (p_i + \cdots + p_j)^2. \tag{2.20}$$

The explicit formula for $n \geq 5$ [2] is

$$F_n^{BDS} = \frac{1}{2}\sum_{i=1}^{n} g_{n,i}, \tag{2.21}$$

where

$$g_{n,i} = -\sum_{r=2}^{[n/2]-1}\log\left(\frac{-t_i^{[r]}}{-t_i^{[r+1]}}\right)\log\left(\frac{-t_{i+1}^{[r]}}{-t_i^{[r+1]}}\right) + D_{n,i} + L_{n,i} + \frac{3}{2}\zeta_2. \tag{2.22}$$

Here D_n and L_n are defined by

$$\begin{aligned} D_{2m+1,i} &= -\sum_{r=2}^{m-1} \mathrm{Li}_2\left(1-\frac{t_i^{[r]}t_{i-1}^{[r+2]}}{t_i^{[r+1]}t_{i-1}^{[r+1]}}\right), \\ L_{2m+1,i} &= -\frac{1}{2}\ln\left(\frac{-t_i^{[m]}}{-t_{i+m+1}^{[m]}}\right)\ln\left(\frac{-t_{i+1}^{[m]}}{-t_{i+m}^{[m]}}\right), \end{aligned} \tag{2.23}$$

for $n = 2m+1$ and

$$\begin{aligned} D_{2m,i} &= -\sum_{r=2}^{m-2} \mathrm{Li}_2\left(1-\frac{t_i^{[r]}t_{i-1}^{[r+2]}}{t_i^{[r+1]}t_{i-1}^{[r+1]}}\right) - \frac{1}{2}\mathrm{Li}_2\left(1-\frac{t_i^{[m-1]}t_{i-1}^{[m+1]}}{t_i^{[m]}t_{i-1}^{[m]}}\right), \\ L_{2m,i} &= -\frac{1}{4}\log\left(\frac{-t_i^{[m]}}{-t_{i+m+1}^{[m]}}\right)\log\left(\frac{-t_{i+1}^{[m]}}{-t_{i+m}^{[m]}}\right), \end{aligned} \tag{2.24}$$

for $n = 2m$. $\mathrm{Li}_2(z)$ denotes the dilogarithm function. The term R_n, called the remainder function, is a function of cross-ratios in momentum space:

$$u_{ijkl} = \frac{x_{ij}^2 x_{kl}^2}{x_{ik}^2 x_{jl}^2}, \quad u_{ijlk} = \frac{x_{ij}^2 x_{kl}^2}{x_{il}^2 x_{jk}^2}, \tag{2.25}$$

which represents a deviation from the BDS formula. The F_n satisfies the anomalous dual conformal identities but the function R_n is itself conformally invariant and is not determined by conformal symmetry.

For the 6-point amplitude [11], the remainder part $R_6 = R_6(u_1, u_2, u_3)$ is a function of the cross-ratios

$$\begin{aligned} u_1 &= \frac{x_{13}^2 x_{46}^2}{x_{14}^2 x_{36}^2} = \frac{t_1^{[2]}t_4^{[2]}}{t_1^{[3]}t_3^{[3]}}, \\ u_2 &= \frac{x_{24}^2 x_{15}^2}{x_{25}^2 x_{14}^2} = \frac{t_2^{[2]}t_1^{[4]}}{t_2^{[3]}t_1^{[3]}}, \\ u_3 &= \frac{x_{35}^2 x_{26}^2}{x_{36}^2 x_{25}^2} = \frac{t_3^{[2]}t_2^{[4]}}{t_3^{[3]}t_2^{[3]}}. \end{aligned} \tag{2.26}$$

The BDS formula of the 6-point amplitude for specific momentum configurations will be discussed in sect. 4.

2.2 Discretized minimal surface

Although exact formula for the minimal surface for $n(\geq 5)$-point amplitudes is not yet known so far, we can study minimal surface by solving numerically the Euler-Lagrange

equations on the square lattice with spacing $h = \frac{2}{M}$ where M is a positive integer. At each site $(-1+hi, -1+hj)$ $(i, j = 0, \cdots, M)$, we assign the variables

$$y_0[i,j] = y_0(-1+hi, -1+hj), \quad r[i,j] = r(-1+hi, -1+hj). \tag{2.27}$$

For the 4-point amplitude, we discretize the differential equations by the central difference method with the boundary conditions

$$\begin{aligned} &y_0[i,0] = y_0(-1+hi, -1), \quad y_0[i,M] = y_0(-1+hi, 1), \\ &y_0[0,j] = y_0(-1, -1+hj), \quad y_0[M,j] = y_0(1, -1+hj), \\ &r[i,0] = r[i,M] = r[0,j] = r[M,j] = 0. \end{aligned} \tag{2.28}$$

Then we obtain $2 \times (M-1)^2$ nonlinear simultaneous equations for $y_0[i,j]$ and $r[i,j]$ and use Newton's method to find a numerical solution. In this paper we use the $M = 520$ lattice data [9], where the Newton method is repeatedly applied until the discrete equation is satisfied up to $\mathcal{O}(10^{-16})$ and the area of the obtained surface does not change up to $\mathcal{O}(10^{-6})$. The area is approximately evaluated as $S = \sum L[i,j]h^2$, where $L[i,j]$ and h are the discretized Lagrangian at a lattice point (i,j) and the lattice spacing, respectively. The area S becomes large as M increases, which is due to the IR divergent behavior near cusps. In [9] we have defined the area of the surface in the radial cut-off regularization

$$S_4^{dis}[r_c] = \sum_{(i,j)\in A[r_c]} L[i,j]h^2, \tag{2.29}$$

where $A[r_c]$ denotes the set of lattice points (i,j) satisfying $r_c[i,j] < r_c$. In this paper, we calculate the area of the conformally boosted minimal surface by evaluating

$$S_4^{dis}[r_c, b] = \sum_{(i,j)\in A[r_c,b]} L[i,j]h^2, \tag{2.30}$$

where $A[r_c, b]$ is made of the points (i,j) satisfying

$$r'[i,j] = \frac{r[i,j]}{1 + by_0[i,j]} < r_c. \tag{2.31}$$

Since it is difficult to estimate the finite r_c correction from the integral formula (2.13) in the case of the 4-point amplitude, we will compare the area (2.30) with numerically evaluated integral (2.13). We can also construct the minimal surface for the 6 and 8-point amplitudes whose boundary conditions are the same as the cut and glue type surface obtained from the 4-point amplitude [9].

r_c	$S_4^{dis}[r_c]$	$S_4[r_c]$	$S_4^{BDS}[r_c]$	$\frac{S_4^{dis}[r_c]-S_4[r_c]}{S_4^{dis}[r_c]}$	$\frac{S_4^{dis}[r_c]-S_4^{BDS}[r_c]}{S_4^{dis}[r_c]}$
0.2	14.6675	14.6086	14.6590	0.004017	0.000581
0.3	10.0349	10.0331	10.12910	0.000179	-0.009392
0.4	7.17606	7.16437	7.31392	0.001630	-0.019211

Table 1: the area of the discretized surface, the integral formula, the BDS amplitudes and their differences (divided by S^{dis}) at $b = 0.0$

3 Numerical check of the minimal surface for the four-point amplitude

In this section, in order to confirm the validity of our numerical approach, we compare the integral formula $S_4[r_c, b]$ for the 4-point amplitude with the area $S_4^{dis}[r_c, b]$ of the discretized minimal surface. We evaluate the area by using $M = 520$ lattice data [9]. The exact radial cut-off area $S_4[r_c, b]$ is evaluated numerically by using Mathematica. We plot $S[r_c, b]$ and $S^{dis}[r_c, b]$ at some values of b (Fig. 1), where we can see that our numerical approach agrees with the exact formula in the region $r_c > 0.2$. In Tables 1 and 2, we compare the values of $S^{dis}[r_c, b]$, $S[r_c, b]$ and $S^{BDS}[r_c, b]$ at $b = 0$, 0.4 by evaluating the ratios $(S_4^{dis}[r_c] - S_4[r_c])/S_4^{dis}[r_c]$ and $(S_4^{BDS}[r_c] - S_4^{dis}[r_c])/S_4^{dis}[r_c]$. Here $S_4^{BDS}[r_c, b]$ is given by dropping the $O(r_c^2 \log r_c^2)$ corrections in (2.16), which is equal to the BDS formula up to the constant term

$$\begin{aligned} S_4^{BDS}[r_c, b] &= \frac{1}{4}\log^2\left(\frac{r_c^2(1-b)^2}{16}\right) + \frac{1}{4}\log^2\left(\frac{r_c^2(1+b)^2}{16}\right) \\ &\quad -\frac{1}{4}\left\{\log\left(\frac{1+b}{1-b}\right)^2\right\}^2 - \frac{\pi^2}{3}. \end{aligned} \tag{3.1}$$

We can see that the discretized minimal surface area agrees with the exact formula for $r_c \geq 0.2$ within 0.2%. It also differs from the BDS formula (3.1) about 2% . The $M = 520$ data numerically reproduces the analytical result of the 4-point amplitude for $r_c \geq 0.2$. From the ratio $(S_4^{BDS} - S^{dis})/S_4^{dis}$, it is found that that finite r_c corrections become small when r_c decreases.

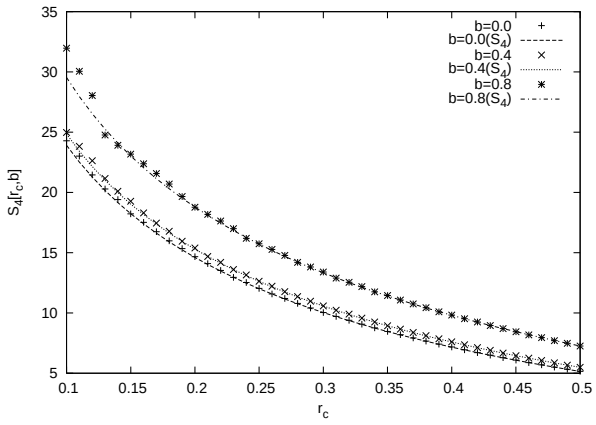

Figure 1: $S_4[r_c, b]$ (lines) and $S_4^{dis}[r_c, b]$ (points) at $b = 0$, 0.4 and 0.8

r_c	$S_4^{dis}[r_c]$	$S_4[r_c]$	$S_4^{BDS}[r_c]$	$\frac{S_4^{dis}[r_c]-S_4[r_c]}{S_4^{dis}[r_c]}$	$\frac{S_4^{BDS}[r_c]-S_4^{dis}[r_c]}{S_4^{dis}[r_c]}$
0.2	15.3943	15.2994	15.3598	0.006166	0.002238
0.3	10.5848	10.5726	10.6886	0.001145	-0.009808
0.4	7.60405	7.59157	7.77310	0.001641	-0.022231

Table 2: the area of the discretized surface, the integral formula, the BDS amplitudes and their differences (divided by S^{dis}) at $b = 0.4$

3.1 Difference of two areas with different b

Since the exact integral formula is known only for the 4-point amplitude, the previous comparison between the numerical result and the analytical expression of the area is only applicable to the case of the 4-point amplitude. We need to find a different approach to estimate the deviation from the BDS formula by reducing the possible finite r_c corrections from the numerical result. In this paper we will consider the difference of two areas with different boost parameter b. Namely we define the function

$$G_4^{dis}[r_c, b] = S_4^{dis}[r_c, b] - S_4^{dis}[r_c, 0]. \tag{3.2}$$

Both terms $S_4^{dis}[r_c, b]$ and $S_4^{dis}[r_c, 0]$ include finite r_c correction. But by taking their difference, some terms of two corrections would cancel each other. In particular b-independent contribution completely vanishes. Then we will compare $G_4^{dis}[r_c, b]$ with the difference of

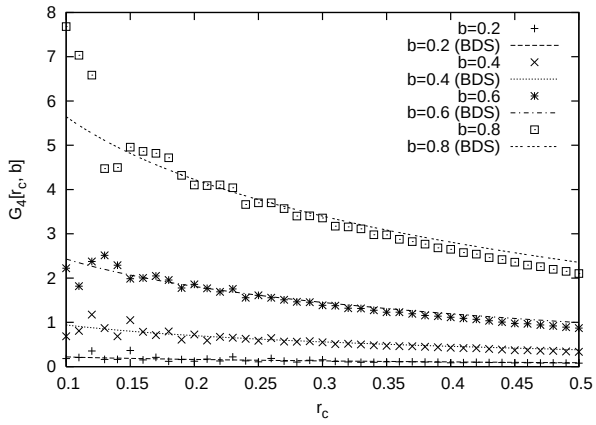

Figure 2: $G_4^{dis}[r_c, b]$ at $b = 0.2$, 0.4, 0.8 ($M = 520$) and $G_4^{BDS}[r_c, b]$

	$r_c = 0.2$	0.3	0.4
$b = 0.2$	-0.327895	0.156186	-0.217681
0.4	0.035675	-0.017397	-0.072860
0.6	0.024418	-0.047297	-0.069778
0.8	-0.03092	-0.012591	-0.061267

Table 3: $\frac{G_4^{dis}[r_c,b]-G_4^{BDS}[r_c,b]}{G_4^{dis}[r_c,b]}$

the corresponding BDS formulas

$$G_4^{BDS}[r_c, b] = S_4^{BDS}[r_c, b] - S_4^{BDS}[r_c, 0]. \tag{3.3}$$

which is also expected to have smaller r_c correction. In Fig. 2, we can see the numerical data is consistent with the BDS formula roughly about $2 - 20\%$ at $r_c = 0.3$ and 0.4 (see Table 3). At $b = 0.2$, the ratio $(G_4^{dis} - G_4^{BDS})/G_4^{dis}$ is large. This is because the ratio is enhanced due to the small value of G_4. Although we can see that there still exist finite r_c corrections, the difference of two areas is a useful method to compare the numerical data with the BDS formula. There are some numerical errors at small r_c due to finite lattice spacing. This error would be improved if we can do more precise calculation at larger M.

4 Numerical test of the six and eight-point amplitudes

We now compare numerical results with the BDS formula for higher-point amplitudes as we did in the end of the previous section. In [9] we constructed numerically the minimal surfaces corresponding to the 6-point and 8-point amplitudes with the same boundary conditions as the surface in [8]. Their boundaries are characterized by the following momenta:

6-point function solution 1:

$$\begin{aligned} 2\pi p_1 &= (2,0,-2), \quad 2\pi p_2 = (-1,0,1), \quad 2\pi p_3 = (1,1,0), \\ 2\pi p_4 &= (-1,0,1), \quad 2\pi p_5 = (1,1,0), \quad 2\pi p_6 = (-2,0,-2). \end{aligned} \tag{4.1}$$

6-point function solution 2:

$$\begin{aligned} 2\pi p_1 &= (1,1,0), \quad 2\pi p_2 = (-1,-1,0), \quad 2\pi p_3 = (2,0,2), \\ 2\pi p_4 &= (-1,1,0), \quad 2\pi p_5 = (1,1,0), \quad 2\pi p_6 = (-2,-2,0). \end{aligned} \tag{4.2}$$

8-point function:

$$\begin{aligned} 2\pi p_1 &= (-1,-1,0), \quad 2\pi p_2 = (1,-1,0), \quad 2\pi p_3 = (-1,0,1), \\ 2\pi p_4 &= (1,0,1), \quad 2\pi p_5 = (-1,0,1), \quad 2\pi p_6 = (1,0,1), \\ 2\pi p_7 &= (-1,1,0), \quad 2\pi p_8 = (1,-1,0). \end{aligned} \tag{4.3}$$

We apply the conformal transformation (2.7) with the boost parameter b and the scale factor a.

4.1 six-point amplitude solution 1

Firstly we consider the solution 1 of the 6-point amplitude. After the conformal transformation, the Mandelstam variables are given by

$$\begin{aligned} &t_1^{[2]} = \frac{4a^2}{1-b}, \ t_2^{[2]} = \frac{4a^2}{(b+1)^2}, \ t_3^{[2]} = 2a^2, \ t_4^{[2]} = \frac{4a^2}{(b+1)^2}, \ t_5^{[2]} = \frac{4a^2}{1-b}, \ t_6^{[2]} = \frac{8a^2}{(b+1)^2}, \\ &t_1^{[3]} = \frac{4a^2}{1-b^2}, \ t_2^{[3]} = \frac{4a^2}{b+1}, \ t_3^{[3]} = \frac{4a^2}{b+1}, \ t_4^{[3]} = \frac{4a^2}{1-b^2}, \ t_5^{[3]} = \frac{4a^2}{b+1}, \ t_6^{[3]} = \frac{4a^2}{b+1}. \end{aligned} \tag{4.4}$$

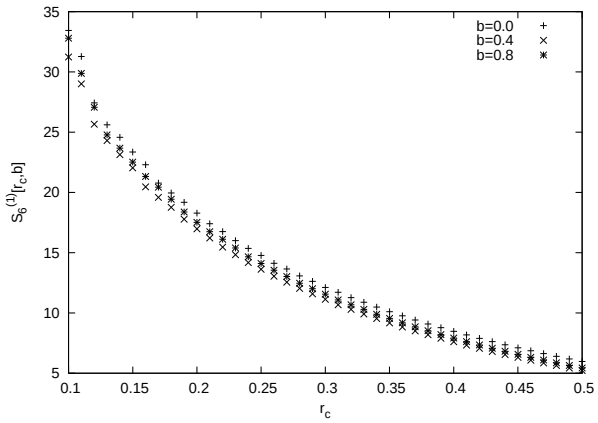

Figure 3: $S_6^{(1)dis}[r_c, b]$ at $b = 0.2$, 0.4, 0.8 ($M = 520$)

Then the cross-ratios are evaluated as

$$u_1 = \frac{t_1^{[2]}t_4^{[2]}}{t_1^{[3]}t_3^{[3]}} = 1, \quad u_2 = \frac{t_2^{[2]}t_1^{[4]}}{t_2^{[3]}t_1^{[3]}} = 1, \quad u_3 = \frac{t_3^{[2]}t_2^{[4]}}{t_3^{[3]}t_2^{[3]}} = 1. \tag{4.5}$$

The cross-rations are independent of b. From the BDS formula (2.19), the amplitude becomes [8]

$$\begin{aligned} S_6^{(1)BDS}[r_c, b] &= \frac{1}{8}\Big\{2\log^2(\frac{r_c^2(1-b)}{8}) + 2\log^2(\frac{r_c^2(1+b)^2}{8}) + \log^2\frac{r_c^2}{4} + \log^2(\frac{r_c^2(1+b)^2}{16})\Big\} \\ &\quad -\frac{1}{2}\Big\{\log 2\log(1-b) - 2\log 2\log(1+b) - 2\log(1-b)\log(1+b) \\ &\quad +\frac{1}{2}\log^2(1-b) + 3\log^2(1+b)\Big\} - \frac{3\pi^2}{16}. \end{aligned} \tag{4.6}$$

Adding the remainder function R_6, the BDS formula is modified as

$$S_6^{(1)}[r_c, b] = S_6^{(1)BDS}[r_c, b] + R_6(1, 1, 1; r_c). \tag{4.7}$$

Here the remainder function depends on the cut-off parameter r_c.

We evaluate $S_6^{(1)dis}[r_c, b]$ from the discretized minimal surface of $M = 520$, which is shown in Fig. 3. Firstly we check whether the BDS conjecture without R_6 term is consistent with the numerical data. In Table 4, we can see small r_c correction from the BDS formula which is 10 times larger than that of the 4-point amplitude. This seems to imply that the remainder function R_6 is non zero. But at this moment we do not

r_c	$S_6^{(1)dis}[r_c]$	$S_6^{(1)BDS}[r_c]$	$\frac{S_6^{(1)dis}[r_c]-S_6^{(1)BDS}[r_c]}{S_6^{(1)dis}[r_c]}$
0.2	16.9788	18.1246	-0.067486
0.3	11.1309	12.3751	-0.11178
0.4	7.61016	8.89403	-0.168705

Table 4: $S_6^{(1)dis}$, $S_6^{(1)BDS}$ and their difference (divided by $S_6^{(1)dis}$) at $b = 0.4$

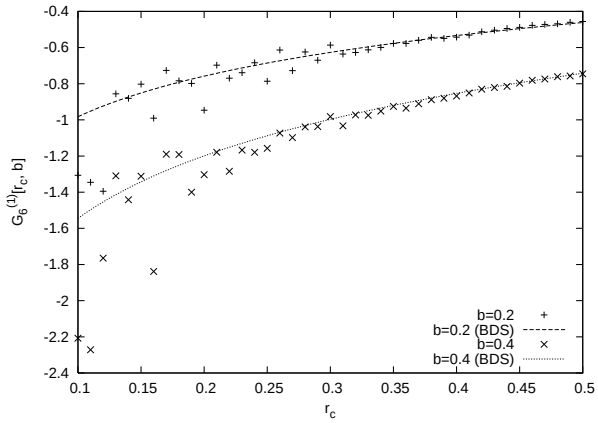

Figure 4: $G_6^{(1)dis}$ and $G_6^{(1)BDS}$ at $b = 0.2$, 0.4

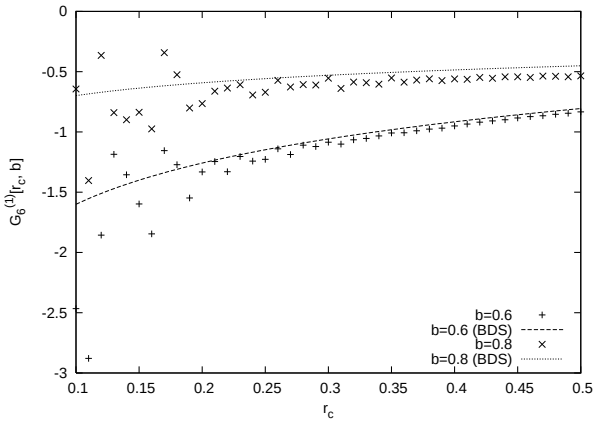

Figure 5: $G_6^{(1)dis}$ and $G_6^{(1)BDS}$ at $b = 0.6$, 0.8

have enough numerical data in order to establish the discrepancy from the BDS formula. Instead we study the difference of two areas with different b, since the effect of the constant factor R_6 is canceled. We define

$$G_6^{(1)dis}[r_c, b] = S_6^{(1)dis}[r_c, b] - S_6^{(1)dis}[r_c, 0], \quad G_6^{BDS(1)}[r_c, b] = S_6^{BDS(1)}[r_c, b] - S_6^{BDS(1)}[r_c, 0]. \tag{4.8}$$

In Figs. 4 and 5, we compare these two functions and find that they behave in a similar manner as we expect from finite r_c corrections in the case of the 4-point amplitude, which is about 10% (Table 5). This table shows that the solution is numerically consistent with the fact that R_6 is independent of b.

	$r_c = 0.2$	0.3	0.4
$b = 0.2$	0.199346	-0.068327	0.016099
0.4	0.079949	-0.015012	0.016734
0.6	0.055443	0.025344	0.036281
0.8	0.225821	0.044057	0.133266

Table 5: $\frac{G_6^{(1)dis}[r_c,b]-G_6^{(1)BDS}[r_c,b]}{G_6^{(1)dis}[r_c,b]}$

4.2 six-point amplitude: solution 2

Secondly we consider the solution 2 of the 6-point amplitude. After the conformal transformation, the Mandelstam variables are

$$t_1^{[2]} = \frac{4a^2}{(1-b)^2},\ \ t_2^{[2]} = \frac{4a^2}{b+1},\ \ t_3^{[2]} = \frac{4a^2}{1-b},\ \ t_4^{[2]} = \frac{4a^2}{(b+1)^2},\ \ t_5^{[2]} = \frac{4a^2}{1-b},\ \ t_6^{[2]} = \frac{4a^2}{b+1},$$
$$t_1^{[3]} = \frac{4a^2}{1-b^2},\ \ t_2^{[3]} = 4a^2,\ \ t_3^{[3]} = \frac{4a^2}{1-b^2},\ \ t_4^{[3]} = \frac{4a^2}{1-b^2},\ \ t_5^{[3]} = 4a^2,\ \ t_6^{[3]} = \frac{4a^2}{1-b^2}. \quad (4.9)$$

The cross-ratios are given by

$$u_1 = \frac{t_1^{[2]}t_4^{[2]}}{t_1^{[3]}t_3^{[3]}} = 1, \quad u_2 = \frac{t_2^{[2]}t_1^{[4]}}{t_2^{[3]}t_1^{[3]}} = 1, \quad u_3 = \frac{t_3^{[2]}t_2^{[4]}}{t_3^{[3]}t_2^{[3]}} = 1, \quad (4.10)$$

which are constants. The BDS formula is given by

$$\begin{aligned} S_6^{BDS(2)}[r_c,b] &= \frac{1}{8}\Big\{\log^2(\frac{r_c^2(1-b)^2}{8}) + \log^2(\frac{r_c^2(1+b)^2}{8}) + 2\log^2(\frac{r_c^2(1+b)}{8}) + 2\log^2(\frac{r_c^2(1-b)}{8})\Big\} \\ &\quad -\frac{1}{2}\Big\{\frac{3}{2}\log^2(1-b) + \frac{3}{2}\log^2(1+b) - 2\log(1-b)\log(1+b)\Big\} - \frac{3\pi^2}{16}. \end{aligned} \quad (4.11)$$

This BDS formula is modified by adding the remainder function $R_6(1,1,1;r_c)$, which is independent of b.

The area $S_6^{(2)dis}[r_c,b]$ from the discretized minimal surface at $M = 520$, which is shown in Fig. 6. For example, the values of $S_6^{(2)dis}[r_c,b]$ and $S_6^{(2)BDS}[r_c,b]$ at $r_c = 0.2$ and $b = 0.4$ is 18.9343 and 19.9554, respectively. The ratio $(S_6^{(2)dis} - S_6^{(2)BDS})/S_6^{(2)dis}$ becomes -0.057218, which is the same order as the case of the 6-point solution 1. We define the

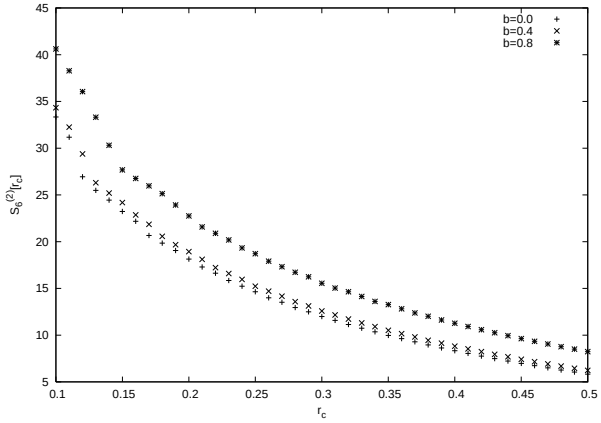

Figure 6: $S_6^{(2)dis}[r_c, b]$ at $b = 0.2,\ 0.4,\ 0.8$ $(M = 520)$

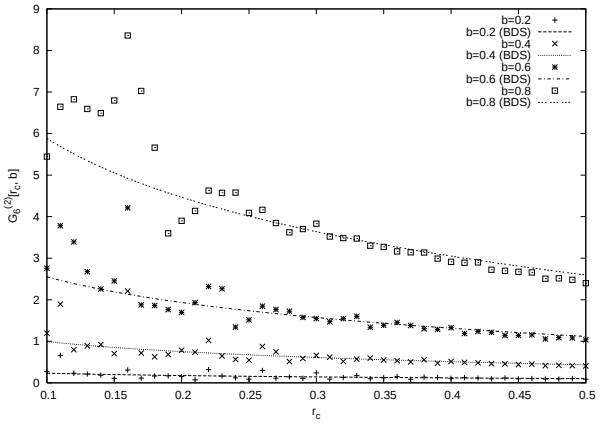

Figure 7: $G_6^{(2)dis}$ and $G_6^{(2)BDS}$ at $b = 0.2$, 0.4, 0.6, 0.8

	$r_c = 0.2$	0.3	0.4
$b = 0.2$	-0.173343	0.406764	-0.084989
0.4	0.040559	0.076990	-0.097516
0.6	-0.140757	-0.016108	0.010283
0.8	-0.145579	0.049971	-0.047002

Table 6: $\frac{G_6^{(2)dis}[r_c,b]-G_6^{(2)BDS}[r_c,b]}{G_6^{(2)dis}[r_c,b]}$

difference functions

$$G_6^{(2)dis}[r_c, b] = S_6^{(2)dis}[r_c, b] - S_6^{(2)dis}[r_c, 0], \quad G_6^{(2)BDS}[r_c, b] = S_6^{(2)BDS}[r_c, b] - S_6^{(2)BDS}[r_c, 0]. \tag{4.12}$$

In Fig. 7 and Table 6, we compare $G_6^{(2)dis}[r_c, b]$ with $G_6^{(2)BDS}[r_c, b]$. Contribution from the remainder function R_6 disappears in $G_6^{(2)dis}$. The difference function from the numerical data is consistent with the BDS formula within 10% at $r_c = 0.4$, which is the same order as we expect from the case of the 4-point solution. This is also consistent with the fact that R_6 for this momentum configuration is independent of b.

4.3 eight-point amplitude

Finally we discuss the 8-point amplitude. After the conformal transformation, the Mandelstam variables are

$$t^{[2]}_{\rm odd} = \frac{4a^2}{(b+1)^2}, \quad t^{[2]}_{\rm even} = 2a^2, \quad t^{[3]}_i = \frac{4a^2}{b+1}, \quad t^{[4]}_{\rm odd} = \frac{8a^2}{(b+1)^2}, \quad t^{[4]}_{\rm even} = 4a^2. \tag{4.13}$$

It is shown that all the values of the cross-ratios u_{ijkl} are independent of b. For example, the cross-ratio

$$u_{1346} = \frac{t^{[2]}_1 t^{[2]}_4}{t^{[3]}_1 t^{[3]}_3} = \frac{\frac{4a^2}{(1+b)^2}2a^2}{\frac{4a^2}{1+b}\frac{4a^2}{1+b}} = \frac{1}{2} \tag{4.14}$$

is constant. The BDS formula for the 8-point amplitude is

$$\begin{aligned} S^{BDS}_8[r_c, b] &= \frac{1}{8}\Big\{4\log^2(\frac{r_c^2(1+b)^2}{8}) + 4\log^2(\frac{r_c^2}{4})\Big\} \\ &\quad -\frac{1}{2}\Big\{4\log^2(1+b) - 4\log 2\log(1+b) - \frac{\pi^2}{6}\Big\} - \frac{\pi^2}{2}. \end{aligned} \tag{4.15}$$

$S_8[r_c, b]$ is obtained by adding the remainder function R_8, which is independent of b.

The area $S^{dis}_8[r_c, b]$ obtained from the discretized minimal surface at $M = 520$, is shown in Fig. 8. For example, at $r_c = 0.2$ and $b = 0.4$, $S^{dis}_8[r_c, b] = 18.8265$ and $S^{BDS}_8[r_c, b] = 17.4285$. The ratio $(S^{dis}_8 - S^{BDS}_8)/S^{dis}_8 = 0.074256$, which is the same order deviation as we observed in the case of 6-point amplitudes. In Fig. 9 and Table 7, we compare two difference functions:

$$G^{dis}_8[r_c, b] = S^{dis}_8[r_c, b] - S^{dis}_8[r_c, 0], \quad G^{BDS}_8[r_c, b] = S^{BDS}_8[r_c, b] - S^{BDS}_8[r_c, 0]. \tag{4.16}$$

We see that R_8-independent G^{dis}_8 obtained from the 8-point discretized minimal surface is consistent with the BDS formula up to finite r_c corrections. This is also consistent with b-independence of the remainder function R_8.

5 Conclusions and discussion

In this paper we studied the area of the minimal surfaces in AdS spacetime surrounded by the light-like boundary which corresponds to the 4, 6 and 8-points gluon scattering amplitudes with specific momentum configurations [8]. For all the solutions, it is found

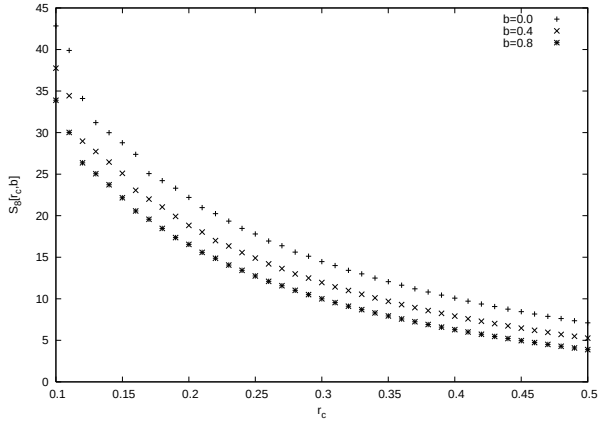

Figure 8: $S_8^{dis}[r_c, b]$ at $b = 0.2$, 0.4, 0.8 ($M = 520$)

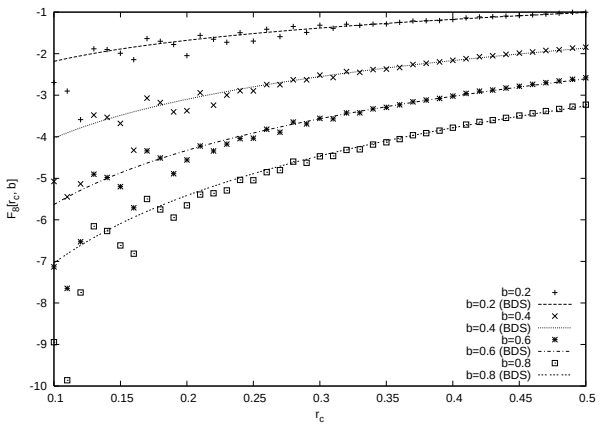

Figure 9: G_8^{dis} and G_8^{BDS} at $b = 0.2$, 0.4, 0.6, 0.8

	$r_c = 0.2$	0.3	0.4
$b = 0.2$	0.179417	-0.052221	0.005237
0.4	0.081445	0.011274	-0.002584
0.6	0.050192	-0.002827	-0.001135
0.8	0.042021	0.002411	-0.000863

Table 7: $\frac{G_8^{dis}[r_c,b]-G_8^{BDS}[r_c,b]}{G_8^{dis}[r_c,b]}$

that the remainder function R_n is independent of b and the R_n-independent difference of the areas with different boost parameters obtained from the discretized minimal surface is consistent with the BDS formula up to finite r_c corrections. It would be interesting to study the 6-point solutions with various momentum configuration (hexagon for example). We can determine numerically the remainder function R_6 as a function of u_1, u_2 and u_3, where at some values we could compare this with the result obtained in [13]. The present numerical approach will be helpful to determine the exact functional form of the remainder function R_n via the AdS/CFT correspondence.

It would be also an interesting problem to estimate the finite r_c correction analytically. The integral formula (2.13) of the 4-point solution can be expanded in r_c and be evaluated

by using hypergeometric function as

$$S_4[r_c, b] = -\frac{2\sqrt{\pi}}{\sqrt{1-b^2r_c^2}} \sum_{n=0}^{\infty} \frac{1}{2n+1}(1-r_c^2)^{n+1} \frac{\Gamma(n+\frac{3}{2})}{\Gamma(2+n)} {}_2F_1(\frac{1}{2}, \frac{3}{2}+n; 2+n; \frac{1-r_c^2}{1-b^2r_c^2}). \tag{5.1}$$

Because of complexity of this formula, it is difficult to estimate the finite r_c corrections at this moment.

Acknowledgments

The authors would like to thank Koh Iwasaki for collaboration in early stage of this work. The work of K. I. is supported in part by the Grant-in-Aid for Scientific Research from Ministry of Education, Science, Culture and Sports of Japan.

References

[1] L. F. Alday and J. Maldacena, "Gluon scattering amplitudes at strong coupling," JHEP **0706** (2007) 064 arXiv:0705.0303 [hep-th].

[2] Z. Bern, L. J. Dixon and V. A. Smirnov, "Iteration of planar amplitudes in maximally supersymmetric Yang-Mills theory at three loops and beyond," Phys. Rev. D **72** (2005) 085001 arXiv:hep-th/0505205.

[3] L. F. Alday, "Lectures on Scattering Amplitudes via AdS/CFT", arXiv:0804.0951 [hep-th]

[4] L. F. Alday and R. Roiban, "Scattering Amplitudes, Wilson Loops and the String/Gauge Theory Correspondence," Phys. Rept. **468**, 153 (2008) arXiv:0807.1889 [hep-th].

[5] S. Abel, S. Forste and V.V. Khoze, "Scattering amplitudes in strongly coupled N=4 SYM from semiclassical strings in AdS", JHEP **0802** (2008) 042, arXiv:[0705.2113] E. I. Buchbinder, "Infrared Limit of Gluon Amplitudes at Strong Coupling," Phys. Lett. **B654** (2007) 46, arXiv: 0706.2015[hep-th].

S. Ryang, " Conformal SO(2,4) Transformations of the One-Cusp Wilson Loop Surface." Phys. Lett. **B659** (2008) 894, arXiv:0710.1673[hep-th]

A. Popolitov, " On coincidence of Alday-Maldacena-regularized sigma-model and Nambu-Goto areas of minimal surfaces", arXiv:0710.2073[hep-th]

G. Yang, " Comment on the Alday-Maldacena solution in calculating scattering amplitude via AdS/CFT", JHEP **0803** (2008) 010, arXiv: 0711.2828[hep-th]

A. Jevicki, K. Jin, C. Kalousios and A. Volovich, " Generating AdS String Solutions", JHEP **0803** (2008) 032, arXiv:0712.1193[hep-th]

Z. Komargodski, " On collinear factorization of Wilson loops and MHV amplitudes in N=4 SYM", JHEP **0805** (2008) 019, arXiv:0801.3274[hep-th]

R. Brower, H. Nastase and H. J.Scnitzer and C.-I. Tan, " Implications of multi-Regge limits for the Bern-Dixon-Smirnov conjecture", arXiv:0801.3891 [hep-th]

A. Mironov, A. Morozov, and T. N. Tomaras, "On n-point Amplitudes in N=4 SYM," JHEP **0711** (2007) 021, arXiv:0708.1625 [hep-th].

A. Mironov and A. Morozov and T. Tomaras, " Some properties of the Alday-Maldacena minimum", Phys. Lett. **B659** (2008) 723, arXiv:0711.0192

H. Itoyama, A. Mironov and A. Morozov, "Boundary Ring: a way to construct approximate NG solutions with polygon boundary conditions: I. Z_n-symmetric configurations," Nucl. Phys. B **808**, 365 (2009) arXiv:0712.0159 [hep-th].

H. Itoyama and A. Morozov, "Boundary Ring or a Way to Construct Approximate NG Solutions with Polygon Boundary Conditions. II. Polygons which admit an inscribed circle," Prog. Theor. Phys. **120**, 231 (2008) arXiv:0712.2316 [hep-th].

Z. Komargodski and S.S Razamat, "Planar quark scattering at strong coupling and universality", JHEP **0801** (2008) 044, arXiv: 0707.4367 [hep-th]

J. McGreevy and A. Sever, "Quark scattering amplitudes at strong coupling," JHEP **0802** (2007) 015, arXiv: 0710.0393[hep-th]

K. Ito, H. Nastase and K. Iwasaki, "Gluon scattering in $\mathcal{N} = 4$ Super Yang-Mills at finite temperature," Prog. Theor. Phys. **120**, 99 (2008) arXiv:0711.3532 [hep-th].

Y. Oz, S. Theisen and S. Yankielowicz, "Gluon Scattering in Deformed N=4 SYM",Phys. Lett. **B662** (2008) 297, arXiv:0712.3491 [hep-th]

M. Kruczenski, "A Note on twist two operators in N=4 SYM and Wilson loops in

Minkowski signature", JHEP **0212** (2002) 024, hep-th/0210115

[6] L. F. Alday and J. Maldacena, "Comments on gluon scattering amplitudes via AdS/CFT," JHEP **0711**, 068 (2007) arXiv:0710.1060 [hep-th].

[7] H. Itoyama, A. Mironov and A. Morozov, "'Anomaly' in n=infinity Alday-Maldacena Duality for Wavy Circle," JHEP **0807**, 024 (2008) arXiv:0803.1547 [hep-th].
D. Galakhov, H. Itoyama, A. Mironov and A. Morozov, "Deviation from Alday-Maldacena Duality For Wavy Circle," arXiv:0812.4702 [hep-th].

[8] D. Astefanesei, S. Dobashi, K. Ito and H. Nastase, "Comments on gluon 6-point scattering amplitudes in N=4 SYM at strong coupling," JHEP **0710** (2007) 077, arXiv:0710.1684[hep-th].

[9] S. Dobashi, K. Ito and K. Iwasaki, "A Numerical Study of Gluon Scattering Amplitudes in N=4 Super Yang-Mills Theory at Strong Coupling", JHEP **0807** (2007) 088, arXiv:0805.3594 [hep-th]

[10] J.M. Drummond, G.P. Korchemsky and E. Sokatchev, "Conformal properties of four-gluon planar amplitudes and Wilson loops", arXiv:0707.0243[hep-th]
A. Brundhuber, P. Heslop and G. Travaglini, "MHV Amplitudes in N=4 Super Yang-Mills and Wilson Loops", Nucl. Phys. **B794** (2008) 231, arXiv:0707:1153[hep-th],
J.M. Drummond, J. Henn, G.P. Korchemsky and E. Sokatchev, "On planar gluon amplitudes/Wilson loops duality", arXiv.0709.2368[hep-th]

[11] J.M. Drummond, J. Henn, G.P. Korchemsky and E. Sokatchev, "Conformal Ward identities for Wilson Loops and a test of the duality with gluon amplitudes", arXiv:0712.1223[hep-th]
J. M. Drummond, J. Henn, G. P. Korchemsky and E. Sokatchev, "Dual superconformal symmetry of scattering amplitudes in N=4 super-Yang-Mills theory," arXiv:0807.1095 [hep-th].

[12] R. Ricci, A. A. Tseytlin and M. Wolf, "On T-Duality and Integrability for Strings on AdS Backgrounds," JHEP **0712** (2007) 082 arXiv:0711.0707 [hep-th].

N. Berkovits and J. Maldacena, "Fermionic T-Duality, Dual Superconformal Symmetry, and the Amplitude/Wilson Loop Connection," JHEP **0809**, 062 (2008) arXiv:0807.3196 [hep-th].

N. Beisert, R. Ricci, A. A. Tseytlin and M. Wolf, "Dual Superconformal Symmetry from AdS5 x S5 Superstring Integrability," Phys. Rev. D **78**, 126004 (2008) arXiv:0807.3228 [hep-th].

[13] J.M. Drummond, J. Henn, G.P. Korchemsky and E. Sokatchev, "Hexagon Wilson Loop=six-gluon MHV amplitude", arXiv:0803.1466[hep-th]

Z. Bern, L.J. Dixon, D.A. Kosower, R. Roiban, M. Spradlin, C. Vergu and A. Volovich, "The Two-Loop Six-Gluon MHV Amplitude in Maximally Supersymmetric Yang-Mills Theory", arXiv:0803.1465[hep-th]